
Assessment of Existing Micro-mechanical Models for Asphalt Mastics Considering Viscoelastic Effects

H.M. Yin* — **W.G. Buttlar**** — **G.H. Paulino****
H. Di Benedetto***

* *Transportation Engineer, Transportation Laboratory
5900 Folsom Boulevard, Sacramento, CA 95819, USA
huiming_yin@dot.ca.gov*

** *University of Illinois at Urbana-Champaign
Department of Civil and Environmental Engineering
205 N. Mathews Ave., Urbana, IL 61801, USA
{buttlar; paulino}@uiuc.edu*

*** *Department Génie Civil et Bâtiment, Laboratory of ENTPE
Rue Maurice Audin, Vaulx-en-Velin, France
herve.dibenedetto@entpe.fr*

ABSTRACT. Micromechanical models have been directly used to predict the effective complex modulus of asphalt mastics from the mechanical properties of their constituents. Because the micromechanics models traditionally employed have been based on elastic theory, the viscoelastic effects of binders have not been considered. Moreover, due to the unique features of asphalt mastics such as high concentration and irregular shape of filler particles, some micromechanical models may not be suitable. A comprehensive investigation of four existing micromechanical methods is conducted considering viscoelastic effects. It is observed that the self-consistent model well predicts the experimental results without introducing any calibration; whereas the Mori-Tanaka model and the generalized self-consistent model, which have been widely used for asphalt materials, significantly underestimate the complex Young's modulus. Assuming binders to be incompressible and fillers to be rigid, the dilute model and the self-consistent model provide the same prediction, but they considerably overestimate the complex Young's modulus. The analyses suggest that these conventional assumptions are invalid for asphalt mastics at low temperatures and high frequencies. In addition, contradictory to the assumption of the previous elastic model, it is found that the phase angle of binders produces considerable effects on the absolute value of the complex modulus of mastics.

KEYWORDS: Asphalt Mastics, Micromechanics, Viscoelasticity, Homogenization, Stress and Strain, Complex Modulus.

DOI:10.3166/RMPD.9.31-57 © 2008 Lavoisier, Paris

1. Introduction

Since the late 1990's, micromechanical models have been introduced to predict effective viscoelastic behavior of asphalt mastics and mixtures from mechanical properties and volume fractions of individual constituents (Buttlar, W.G., and R. Roque 1996, Buttlar *et al.*, 1999; Shashidhar and Shenoy, 2002; Kim *et al.*, 2004). Because those micromechanical models are based on purely elastic solutions (Mura, 1987), absolute value of complex modulus is directly taken as elastic modulus to use the same formulae. Thus, they can only provide the absolute value of effective complex modulus of asphalt materials but cannot predict the phase angle. However, because asphalt binders exhibit viscoelastic behavior with a varying complex modulus over a large range of frequencies, viscoelastic models are needed to gain better insight into effective viscoelastic properties of asphalt materials considering phase angles and frequency dependent properties (Kim *et al.*, 2004).

Eshelby's pioneering work (Eshelby, 1957; Eshelby, 1959) on elastic solutions for an infinite medium including a single inclusion provides a solid foundation for micromechanical models. Eshelby (1957) has pointed out that the elastic theory of inclusions can be extended to viscoelastic materials. Typically, the viscoelastic problem is reformulated in the Fourier or Laplace domain *via* the elastic-viscoelastic correspondence principle (Fung, 1965; Christensen, 1982; Kim *et al.*, 1995; Paulino and Jin, 2001; Mukherjee and Pau, 2003) and then solved in accordance with the corresponding elastic problem. Hashin (1965, 1970) developed a correspondence principle which relates effective elastic moduli of composites to effective relaxation moduli and creep compliances of viscoelastic composites. Christensen (1969) derived two bounds for the effective viscoelastic mechanical properties of two-phase mixtures. Subsequently, the self-consistent method (Hill 1965; Budiansky 1965), the Hashin-Shtrikman bounds (Hashin. and Shtrikman, 1963), and the Mori-Tanaka model (Mori and Tanaka, 1973) have been extended to viscoelastic composites (Laws and McLaughlin, 1978, Gibiansky and Milton, 1993; Milton and Berryman, 1997; Brinson and Lin, 1998). In recent years, micromechanics-based viscoelastic models have been proposed to interpret the nonlinear viscoelastic and viscoplastic behavior of composites (Li and Weng, 1998; Ponte Castaneda and Suquet, 1998; Haj-Ali and Muliana, 2003).

Asphalt mastics are generally considered to contain asphalt binders and filler particles no larger than 75 microns (Buttlar *et al.*, 1999; Palade *et al.*, 2000; Airey *et al.*, 2004; Abbas *et al.*, 2004). The viscoelastic properties of an asphalt mastic will strongly influence the viscoelastic behavior of the asphalt concrete paving mixture which it resides in, which in turn will strongly influence pavement performance. To characterize the viscoelastic behavior of asphalt mastics, several experimental devices have been employed such as the bending beam rheometer, the dynamic shear rheometer (DSR), and the hollow cylinder tester (Anderson *et al.*, 1994; Buttlar *et al.*, 2002). Because asphalt binders generally exhibit viscous behavior and filler particles are much stiffer than binders, conventionally asphalt binders are

assumed to be incompressible and filler particles are assumed to be rigid. Thus, the mastics are also incompressible. Due to the assumptions of the isotropy and incompressibility, only one independent parameter is needed to describe the material properties of asphalt mastics. Therefore, most experimental efforts aim at obtaining the complex shear modulus (Anderson *et al.*, 1994; Buttlar *et al.*, 1999; Shashidhar and Shenoy, 2002).

Due to its relatively low cost and good repeatability, the DSR test has become a popular measurement device for mastics containing very small particles. During the testing, sinusoidal loading is provided and stress-strain relations are obtained at different frequencies and temperatures. The stress-strain relation can be represented either by absolute value and phase angle of complex modulus or by storage modulus and loss modulus. Using time-temperature superposition, master curves for the absolute value and phase angle of complex modulus are generated at a specific temperature (Ferry, 1980). Then, employing the Fourier transform, the master curve of relaxation modulus or creep compliance can be further developed (Park and Kim 1999). Obviously, mastics with different filler volume fractions should produce different master curves.

Because effective material behavior of composites not only depends upon the physical properties of each constituent but also depend upon the microstructural aspects, such as particle shape and distribution (Masad *et al.*, 1999; You and Buttlar, 2004; Little and Petersen, 2005; Lackner *et al.*, 2005), specific micromechanical models have advantages for specific composites due to the particular simplifications and assumptions made. Although several micromechanical models have been employed in predicting effective elastic properties of asphalt mastics and mixtures, some additional phenomenological parameters or calibrations have been introduced to fit experiments. Moreover, viscoelastic behavior of asphalt binders has not been addressed.

The purpose of this paper is to develop a micromechanics-based model to obtain effective viscoelastic properties of asphalt mastics with changing volume concentration of filler. Given an asphalt mastic sample with known complex modulus of the binder and the elastic modulus of the filler, a uniform sinusoidal force is applied on its boundary. Based on various micromechanics-based homogenization methods (Yin and Sun, 2005; Christensen and Lo, 1979), particle and matrix's averaged strains are obtained, and thus the effective stress and strain relation is provided. In this paper, four micromechanics-based models are presented, as follows:

- The dilute model (DM);
- The self-consistent model (SCM);
- The Mori-Tanaka model (MTM);
- The generalized self-consistent model (GSCM).

The difference between these models and limitations of each model are presented, and applicability of these models to asphalt mastics is discussed. To assess the validity of the four models, comparisons with experimental data are provided without introducing any calibration to the models. Using SCM, master curves of complex moduli of asphalt mastics is generated and compared with experiments. The remainder of this paper presents a detailed description of the viscoelastic models, a cross-comparison between the models, comparison with experimental results, and finally, parametric analyses of effective material behavior of mastics.

2. Viscoelastic solution for a single particle embedded in an infinite binder medium

A particulate composite consists of many discrete particles embedded in a continuous matrix. To test the effective elastic properties, a uniform stress field is applied on the boundary. From the relation between the averaged deformation and the applied loading, effective stiffness is derived. The calculation is typically based on the solution for one particle, which may have more than one surface layers, embedded in an elastic matrix (Christensen and Lo, 1979; Herve and Zaoui, 1993). For viscoelastic composites, a uniform sinusoidal loading is applied on the boundary. From the overall response of the composite, the effective viscoelastic properties can be obtained in a similar fashion, and the solution for one particle embedded in a viscoelastic matrix must be provided.

Consider a single particle embedded in an infinite viscoelastic binder under a uniform sinusoidal stress field as $\tilde{\boldsymbol{\sigma}}^0 e^{i2\pi\omega t}$, where ω denotes the frequency of the loading, and $\tilde{\boldsymbol{\sigma}}^0$ the applied loading in the frequency domain. In what follows, the quantities in the frequency domain are denoted by the over-tilde. The stiffness of the fillers and the binder are denoted by \mathbf{C}^1 and $\mathbf{C}^0(t)$, respectively. Here the particle is elastic, but the binder is viscoelastic, and thus, the stiffness (relaxation modulus) is time-dependent. The constitutive law for the binder can be given in terms of a Stieltjes integral equation with the form (Christensen, 1982) as

$$\boldsymbol{\sigma}(\mathbf{r}, t) = \int_{-\infty}^t \mathbf{C}^0(t - \tau) : \frac{\partial \boldsymbol{\varepsilon}(\mathbf{r}, \tau)}{\partial \tau} d\tau, \quad \mathbf{r} \in D - \Omega, \quad [1]$$

where D and Ω denote the infinite domain and the particle domain, respectively. The tensor operations of “:” and “.” follow the standard rules (Nemat-Nasser and Hori, 1999). At steady state, the local mechanical fields can be written in a separable form as

$$\boldsymbol{\varepsilon}(\mathbf{r}, t) = \tilde{\boldsymbol{\varepsilon}}(\mathbf{r}) e^{i2\pi\omega t}; \quad \boldsymbol{\sigma}(\mathbf{r}, t) = \tilde{\boldsymbol{\sigma}}(\mathbf{r}) e^{i2\pi\omega t} \quad [2]$$

Substitution of Equation [2] into Equation [1] provides

$$\tilde{\boldsymbol{\sigma}}(\mathbf{r}) = \tilde{\mathbf{C}}^0 : \tilde{\boldsymbol{\varepsilon}}(\mathbf{r}), \quad [3]$$

in which

$$\tilde{\mathbf{C}}^0 = i2\pi\omega \int_0^{\infty} \mathbf{C}^0(\tau) e^{-i2\pi\omega\tau} d\tau. \quad [4]$$

In general, both fillers and binders for asphalt mastics are considered as isotropic materials. Therefore, the fourth rank tensors \mathbf{C}^1 and $\tilde{\mathbf{C}}^0$ can be described by two independent components of bulk modulus and shear modulus, written as k^1 and μ^1 , and \tilde{k}^0 and $\tilde{\mu}^0$, respectively. Because the bulk modulus of asphalt cements is generally much higher than the shear modulus, asphalt cements can be approximated to be incompressible materials (Anderson *et al.*, 1994). Consequently, only shear modulus needs to be measured. Once the complex tensor $\tilde{\mathbf{C}}^0$ is obtained as a function of frequencies, through Equation [4], we can inversely derive the relaxation modulus and then creep compliance (Park and Kim, 1999).

If no particle exists in the medium, from Equation [3] the strain field is obviously uniform. However, due to the existence of the inhomogeneity, the stress and strain fields in the neighborhood of the particle are disturbed. Eshelby (1957, 1959) proposed an equivalent inclusion method to solve this problem. First, the particle is assumed to be same as the binder material, and the uniform strain field is obtained. Next, an eigenstrain is introduced in the particle domain to simulate the material mismatch between the particle and the binder, and is chosen to make the stress in the particle domain equivalent to the one on the real particle. Finally, the strain field in the total domain can be exactly obtained (Mura, 1987). Appendix A provides a detailed derivation of this solution. It can be found that the strain in the particle domain is still uniform, which can be written as

$$\tilde{\boldsymbol{\varepsilon}}^\Omega = \tilde{\boldsymbol{\varepsilon}}^0 - \mathbf{P}^0 \cdot (\mathbf{P}^0 - \Delta\tilde{\mathbf{C}}^{-1})^{-1} : \tilde{\boldsymbol{\varepsilon}}^0, \quad [5]$$

where the fourth rank tensor \mathbf{P}^0 is defined in Appendix A (see Equation [43]).

It is noted that, for an elliptical particle embedded in an infinite viscous matrix, the stress and strain fields can also be solved from Eshelby's solution. Gilormin and Montheillet (1986) derived the solution and proposed the application in modeling damage of the materials. For a one-layered spherical particle embedded in an infinite binder under shear loading, the local strain can also be derived from the elastic solution (Christensen and Lo, 1979).

3. Viscoelastic formulation of four micromechanical models

Consider an asphalt mastic containing an infinite number of filler particles dispersed in a viscoelastic binder. To test the effective viscoelastic properties, a uniform sinusoidal stress field $\tilde{\boldsymbol{\sigma}}^0 e^{i2\pi\omega t}$ is applied on the boundary of the composite. The particles and binder have the materials properties also denoted by \mathbf{C}^1 and $\tilde{\mathbf{C}}^0$, respectively. Notice that herein the elastic tensor \mathbf{C}^1 is constant, whereas the viscoelastic tensor $\tilde{\mathbf{C}}^0$ is a complex matrix, which depends on the frequency and can be represented by two independent complex components of bulk modulus and shear modulus. Based on the equilibrium in absence of the inertial force, the averaged stress of the composite in the frequency domain can be written as (Yin and Sun, 2005; Mura, 1987):

$$\langle \tilde{\boldsymbol{\sigma}} \rangle_D = \tilde{\boldsymbol{\sigma}}^0, \quad [6]$$

where the angle bracket with subscript D denotes the volume average over the total mastic. In what follows, we use subscripts D , Ω , and M to represent the mastic, filler, and binder domains, respectively. Because filler particles are fully bonded to the matrix, the averaged stress and strain of the mastic contain the contributions from the two phases as:

$$\langle \tilde{\boldsymbol{\sigma}} \rangle_D = \phi \mathbf{C}^1 : \langle \tilde{\boldsymbol{\varepsilon}} \rangle_\Omega + (1 - \phi) \tilde{\mathbf{C}}^0 : \langle \tilde{\boldsymbol{\varepsilon}} \rangle_M, \quad [7]$$

$$\langle \tilde{\boldsymbol{\varepsilon}} \rangle_D = \phi \langle \tilde{\boldsymbol{\varepsilon}} \rangle_\Omega + (1 - \phi) \langle \tilde{\boldsymbol{\varepsilon}} \rangle_M. \quad [8]$$

where ϕ denotes the volume fraction of filler particles. Given the averaged stress, if the averaged strain of the composite can also be solved, the relation between stress and strain can be obtained. Because the mastic contains numerous particles and the microstructure varies randomly, it is not feasible to formulate an exact local solution. Fortunately, to obtain the effective stress-strain relation, only the averages of stress and strain are needed. Some homogenization methods are proposed to solve for the particle averaged strain based on the solution for one particle embedded in the infinite domain. Different homogenization methods lead to different micromechanical models (Yin and Sun, 2005). In what follows, we formulate four micromechanical models: the dilute model (DM), the Mori-Tanaka model (MTM), the self-consistent model (SCM), and the generalized self-consistent model (GSCM).

3.1. Dilute model

For a dilute distribution of particles in a viscoelastic matrix, because the distance between particles is much larger than the radius of particles, the particle

interactions can be disregarded (Nemat-Nasser and Hori, 1999). The particle's averaged strain can be directly obtained from the local solution in Equation [5] as

$$\langle \tilde{\boldsymbol{\varepsilon}} \rangle_{\Omega} = (\mathbf{I} - \mathbf{P}^0 \cdot \Delta \tilde{\mathbf{C}})^{-1} \cdot (\tilde{\mathbf{C}}^0)^{-1} : \tilde{\boldsymbol{\sigma}}^0 . \quad [9]$$

Combining Equations [7]-[9], we can write the averaged strain as

$$\langle \tilde{\boldsymbol{\varepsilon}} \rangle_D = (\tilde{\mathbf{C}}^0)^{-1} : \tilde{\boldsymbol{\sigma}}^0 - \phi (\tilde{\mathbf{C}}^0)^{-1} \cdot \Delta \tilde{\mathbf{C}} \cdot (\mathbf{I} - \mathbf{P}^0 \cdot \Delta \tilde{\mathbf{C}})^{-1} \cdot (\tilde{\mathbf{C}}^0)^{-1} : \tilde{\boldsymbol{\sigma}}^0 . \quad [10]$$

Comparing the averaged stress and strain in Equations [6] and [10], we obtain the effective complex stiffness (Nemat-Nasser and Hori, 1999; Yin and Sun, 2005) as

$$\langle \tilde{\mathbf{C}} \rangle_D = \tilde{\mathbf{C}}^0 \cdot \left[\mathbf{I} + \phi (\tilde{\mathbf{C}}^0)^{-1} \cdot (\mathbf{P}^0 - \Delta \tilde{\mathbf{C}}^{-1}) \right]^{-1} . \quad [11]$$

Because all the tensors in the above equation are isotropic, the effective complex stiffness can be denoted by complex bulk modulus and shear modulus as

$$\langle \tilde{k} \rangle_D = \tilde{k}^0 + \frac{\phi \tilde{k}^0}{\frac{\tilde{k}^0}{k^1 - \tilde{k}^0} + \frac{3\tilde{k}^0}{3\tilde{k}^0 + 4\tilde{\mu}^0} - \phi}; \quad \langle \tilde{\mu} \rangle_D = \tilde{\mu}^0 + \frac{\phi \tilde{\mu}^0}{\frac{\tilde{\mu}^0}{\mu^1 - \tilde{\mu}^0} + \frac{6\tilde{k}^0 + 2\tilde{\mu}^0}{5\tilde{k}^0 + 4\tilde{\mu}^0} - \phi} . \quad [12]$$

Assuming the particles to be rigid, namely $k^1 \gg |\tilde{k}^0|$ and $\mu^1 \gg |\tilde{\mu}^0|$, the above equation is reduced into

$$\langle \tilde{k} \rangle_D = \tilde{k}^0 + \frac{\phi \tilde{k}^0}{\frac{3\tilde{k}^0}{3\tilde{k}^0 + 4\tilde{\mu}^0} - \phi}; \quad \langle \tilde{\mu} \rangle_D = \tilde{\mu}^0 + \frac{\phi \tilde{\mu}^0}{\frac{6\tilde{k}^0 + 2\tilde{\mu}^0}{5\tilde{k}^0 + 4\tilde{\mu}^0} - \phi} . \quad [13]$$

Further assuming the binder to be incompressible (Christensen and Anderson, 1992), namely $|\tilde{k}^0| \gg |\tilde{\mu}^0|$, Equation [13] can be rewritten as

$$\langle \tilde{k} \rangle_D = \frac{\tilde{k}^0}{1 - \phi}; \quad \langle \tilde{\mu} \rangle_D = \frac{\tilde{\mu}^0}{1 - 2.5\phi} . \quad [14]$$

Because the dilute distribution of particles is assumed, this model is only valid for mastics with small volume fractions of fillers. When volume fraction ϕ increases to a certain value, the results can be divergent because the denominators in the above equation may reduce to zero (for instance, as volume fraction $\phi \rightarrow 0.4$, Equation [14] is found to diverge).

3.2. Mori-Tanaka model

The Mori-Tanaka model (MTM) involves complex manipulations of the field variables in Mori and Tanaka (1973). Yin and Sun (2005) proposed a more straightforward method to derive this model. In this method, a particle is embedded into the matrix with a uniform strain same as the matrix's averaged strain, and the particle's averaged strain is calculated from the solution for one particle embedded in the infinite matrix in Equation [5] as

$$\langle \tilde{\boldsymbol{\varepsilon}} \rangle_{\Omega} = (\mathbf{I} - \mathbf{P}^0 \cdot \Delta \tilde{\mathbf{C}})^{-1} : \langle \tilde{\boldsymbol{\varepsilon}} \rangle_M. \quad [15]$$

Combining Equations [15] with [7] and [8] provides the effective complex stiffness (Yin and Sun, 2005) as:

$$\langle \tilde{\mathbf{C}} \rangle_D = \tilde{\mathbf{C}}^0 + \phi [\Delta \tilde{\mathbf{C}}^{-1} - (1 - \phi) \mathbf{P}^0]^{-1}. \quad [16]$$

Then the effective complex bulk modulus and shear modulus can be written as

$$\langle \tilde{k} \rangle_D = \tilde{k}^0 + \frac{\phi \tilde{k}^0}{\frac{\tilde{k}^0}{k^1 - \tilde{k}^0} + \frac{3(1 - \phi) \tilde{k}^0}{3\tilde{k}^0 + 4\tilde{\mu}^0}}; \langle \tilde{\mu} \rangle_D = \tilde{\mu}^0 + \frac{\phi \tilde{\mu}^0}{\frac{\tilde{\mu}^0}{\mu^1 - \tilde{\mu}^0} + \frac{6(1 - \phi)(\tilde{k}^0 + 2\tilde{\mu}^0)}{5(3\tilde{k}^0 + 4\tilde{\mu}^0)}}. \quad [17]$$

In the case of perfectly rigid particles, the above equation reduces to

$$\langle \tilde{k} \rangle_D = \frac{\tilde{k}^0}{1 - \phi} + \frac{4\phi \tilde{\mu}^0}{3(1 - \phi)}; \langle \tilde{\mu} \rangle_D = \tilde{\mu}^0 + \frac{5\phi \tilde{\mu}^0 (3\tilde{k}^0 + 4\tilde{\mu}^0)}{6(1 - \phi)(\tilde{k}^0 + 2\tilde{\mu}^0)}. \quad [18]$$

Finally for the case of a nearly incompressible matrix phase, Equation [18] becomes

$$\langle \tilde{k} \rangle_D = \frac{\tilde{k}^0}{1 - \phi}; \langle \tilde{\mu} \rangle_D = \frac{(1 + 1.5\phi) \tilde{\mu}^0}{1 - \phi}. \quad [19]$$

It is found that the expression of the effective bulk modulus is in the same form as Equation [14]. However, the effective shear modulus is different. It is noted that the divergent problem will not exist in Equation [19] except for $\phi = 1$, where the effective stiffness is supposed to be infinite.

3.3. Self-consistent model

In the self-consistent model (SCM), any material point on the fillers is isolated as an infinitesimal volume element. Then, the rest of the material is homogenized as a uniform material, whose mechanical property is identical to the mastic itself. The particle averaged strain is derived from the solution for one particle embedded in the infinite domain which has the same material properties as the mastic (Hill, 1965; Budiansky, 1965) as:

$$\langle \tilde{\boldsymbol{\varepsilon}} \rangle_{\Omega} = \left[\mathbf{I} - \bar{\mathbf{P}}^0 \cdot \left(\mathbf{C}^1 - \langle \tilde{\mathbf{C}} \rangle_D \right) \right]^{-1} : \langle \tilde{\boldsymbol{\varepsilon}} \rangle_D \quad [20]$$

where $\bar{\mathbf{P}}^0$ depends on the material properties of the mastic instead of those of the binder, namely,

$$\bar{P}_{ijkl}^0 = \frac{1}{15\langle \tilde{\mu} \rangle_D} \left[\frac{3\langle \tilde{k} \rangle_D + \langle \tilde{\mu} \rangle_D}{3\langle \tilde{k} \rangle_D + 4\langle \tilde{\mu} \rangle_D} \delta_{ij} \delta_{kl} - \frac{9}{2} \frac{\langle \tilde{k} \rangle_D + 2\langle \tilde{\mu} \rangle_D}{3\langle \tilde{k} \rangle_D + 4\langle \tilde{\mu} \rangle_D} (\delta_{ik} \delta_{jl} + \delta_{il} \delta_{jk}) \right]. \quad [21]$$

Combination of Equations [20] with [7] and [8] yields the averaged stress-strain relation as

$$\langle \tilde{\boldsymbol{\sigma}} \rangle_D = \left\{ \tilde{\mathbf{C}}^0 + \phi \left(\mathbf{C}^1 - \tilde{\mathbf{C}}^0 \right) \cdot \left[\mathbf{I} - \bar{\mathbf{P}}^0 \cdot \left(\mathbf{C}^1 - \langle \tilde{\mathbf{C}} \rangle_D \right) \right]^{-1} \right\} : \langle \tilde{\boldsymbol{\varepsilon}} \rangle_D. \quad [22]$$

Thus, the effective complex stiffness (Nemat-Nasser and Hori, 1999; Yin and Sun, 2005) is obtained as:

$$\langle \tilde{\mathbf{C}} \rangle_D = \tilde{\mathbf{C}}^0 + \phi \left(\mathbf{C}^1 - \tilde{\mathbf{C}}^0 \right) \cdot \left[\mathbf{I} - \bar{\mathbf{P}}^0 \cdot \left(\mathbf{C}^1 - \langle \tilde{\mathbf{C}} \rangle_D \right) \right]^{-1}. \quad [23]$$

It is noted that here $\langle \tilde{\mathbf{C}} \rangle_D$ is implicitly given and it should be generally solved by the recursive method. For isotropic materials, the effective complex bulk and shear moduli are further written as

$$\begin{aligned} \langle \tilde{k} \rangle_D &= \tilde{k}^0 + \frac{\phi(k^1 - \tilde{k}^0)(3\langle \tilde{k} \rangle_D + 4\langle \tilde{\mu} \rangle_D)}{3k^1 + 4\langle \tilde{\mu} \rangle_D} \\ \langle \tilde{\mu} \rangle_D &= \tilde{\mu}^0 + \frac{5\phi(\mu^1 - \tilde{\mu}^0)\langle \tilde{\mu} \rangle_D(3\langle \tilde{k} \rangle_D + 4\langle \tilde{\mu} \rangle_D)}{6\mu^1(\langle \tilde{k} \rangle_D + 2\langle \tilde{\mu} \rangle_D) + \langle \tilde{\mu} \rangle_D(9\langle \tilde{k} \rangle_D + 8\langle \tilde{\mu} \rangle_D)}. \end{aligned} \quad [24]$$

To numerically obtain the effective material properties, the effective complex bulk and shear moduli can be initialized as $\langle \tilde{k} \rangle_D = \tilde{k}^0$ and $\langle \tilde{\mu} \rangle_D = \tilde{\mu}^0$. Substituting these values into the right side of the above equations updates the effective complex moduli until that they are convergent. Thus, the effective viscoelastic moduli are obtained.

However, for rigid particles, the effective complex shear modulus can be explicitly solved as

$$\langle \tilde{\mu} \rangle_D = \frac{4(3-\phi)\tilde{\mu}^0 - 3(2-5\phi)\tilde{k}^0 + \sqrt{[4(3-\phi)\tilde{\mu}^0 - 3(2-5\phi)\tilde{k}^0]^2 - 288(2\phi-1)\tilde{\mu}^0\tilde{k}^0}}{24(1-2\phi)}, \quad [25]$$

and the effective bulk modulus is obtained as

$$\langle \tilde{k} \rangle_D = \frac{3\tilde{k}^0 + 4\phi\langle \tilde{\mu} \rangle_D}{3(1-\phi)}. \quad [26]$$

If the matrix is nearly incompressible, the effective complex bulk and shear modulus can be further simplified into

$$\langle \tilde{k} \rangle_D = \frac{\tilde{k}^0}{1-\phi}; \quad \langle \tilde{\mu} \rangle_D = \frac{\tilde{\mu}^0}{1-2.5\phi}. \quad [27]$$

which is the same as Equation [14].

3.4. Generalized self-consistent model

The generalized self-consistent model (GSCM) is derived from the solution for a spherical particle embedded in a concentric spherical annulus of the binder of the prescribed volume fraction, which in turn is embedded in an infinite medium with the effective mechanical properties of the mastic (Christensen and Lo, 1979). Because the viscoelastic solution in the frequency domain can also be obtained in the same fashion, the effective complex shear modulus should satisfy the following quadratic equation:

$$A \left(\frac{\langle \tilde{\mu} \rangle_D}{\tilde{\mu}^0} \right)^2 + 2B \left(\frac{\langle \tilde{\mu} \rangle_D}{\tilde{\mu}^0} \right) + C = 0, \quad [28]$$

where A , B , and C are related to viscoelastic moduli of each phase and the volume fraction. The detailed expressions of these parameters are seen in Christensen (Christensen, 1990). The effective complex bulk modulus is the same as the one of the MTM in Equation [17].

In the case of perfectly rigid particles, the parameters can be simplified as

$$\begin{aligned}
 A &= 8(4 - 5\tilde{v}^0)(7 - 10\tilde{v}^0)\phi^{10/3} - 50[7 - 12\tilde{v}^0 + 8(\tilde{v}^0)^2]\phi^{7/3} + 252\phi^{5/3} \\
 &\quad - 50[7 - 12\tilde{v}^0 + 8(\tilde{v}^0)^2]\phi + 8(4 - 5\tilde{v}^0)(7 - 10\tilde{v}^0), \\
 B &= -2(1 - 5\tilde{v}^0)(7 - 10\tilde{v}^0)\phi^{10/3} + 50[7 - 12\tilde{v}^0 + 8(\tilde{v}^0)^2]\phi^{7/3} - 252\phi^{5/3} \\
 &\quad + 75(3 - \tilde{v}^0)\tilde{v}^0\phi - 3(4 - 5\tilde{v}^0)(7 - 15\tilde{v}^0), \\
 C &= -4(7 - 5\tilde{v}^0)(7 - 10\tilde{v}^0)\phi^{10/3} - 50[7 - 12\tilde{v}^0 + 8(\tilde{v}^0)^2]\phi^{7/3} + 252\phi^{5/3} \\
 &\quad - 25[7 - (\tilde{v}^0)^2]\phi - 2(4 - 5\tilde{v}^0)(7 + 5\tilde{v}^0),
 \end{aligned} \tag{29}$$

where the complex Poisson's ratio is written as $\tilde{v}^0 = (3\tilde{k}^0 - 2\tilde{\mu}^0)/(6\tilde{k}^0 + 2\tilde{\mu}^0)$.

For the case of a nearly incompressible matrix phase, the Poisson's ratio is written $\tilde{v}^0 \rightarrow 0.5$. Then the parameters further reduce to

$$\begin{aligned}
 A &= 24\phi^{10/3} - 150\phi^{7/3} + 252\phi^{5/3} - 150\phi + 24, \\
 B &= 6\phi^{10/3} + 150\phi^{7/3} - 252\phi^{5/3} + 93.75\phi + 2.25, \\
 C &= -36\phi^{10/3} - 150\phi^{7/3} + 252\phi^{5/3} - 168.75\phi - 28.5.
 \end{aligned} \tag{30}$$

For each case, from Equation [28], the effective shear modulus is obtained as

$$\langle \tilde{\mu} \rangle_D = \frac{\sqrt{B^2 - AC} - B}{A} \tilde{\mu}^0. \tag{31}$$

In summary, for the four models, the complex bulk modulus and shear modulus are given for three cases:

- elastic filler particles and compressible viscoelastic binders;
- rigid filler particles and compressible viscoelastic binders, and;
- rigid filler particles and incompressible viscoelastic binders.

Although these models have been successfully used to predict the elastic behavior of many heterogeneous materials, because asphalt mastics contain a unique microstructure and exhibit strong viscoelastic behavior, the applicability of these models requires validation.

4. Simplifications and limitations of four models

In a mastic as seen in Figure 1a, the size, shape, and distribution of the filler particles are uncertain, so the microstructure of the mastic is considered to be statistically random. Given a sinusoidal loading $\tilde{\sigma}^0$ uniformly on the boundary, the strain field in the mastic depends on the microstructure. It is difficult to obtain the effective material properties based on a specific many-particle configuration, moreover, which may not be applicable to the general cases. Therefore, researchers have pursued analytical solution using some specific assumptions. Essentially, all above micromechanical models are based the solution for one particle embedded the matrix, and thus have some limitations.

In Figure 1b, DM simply disregards the effect of other particles and assumes the highlighted particle (white particles) to be spherical. Then, the particle averaged strain is obtained by one particle embedded in the binder under the uniform loading $\tilde{\sigma}^0$. Obviously, the particle interaction and the effect of the particle shape are not considered. Therefore, this model is only applicable for composites with very low volume fraction of spherical particles.

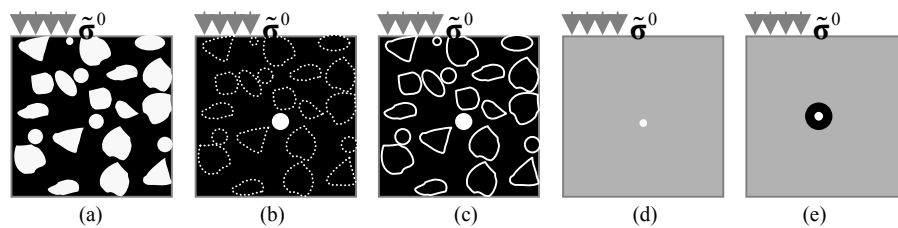


Figure 1. Schematic illustration for estimating averaged strain of the particle phase by four micromechanical models. (a) The actual mastic under external loading; (b) the dilute model; (c) the Mori-Tanaka model; (d) the self-consistent model, and; (e) the generalized self-consistent model

In Figure 1c, before the highlighted particle is embedded in the binder, due to the existence of other particles, the strain field surrounding the highlighted particle is greatly distorted. The MTM assumes the strain field in the neighborhood of the particle to be uniform, which is denoted by the binder averaged strain. When the particle is embedded in the binder, the particle averaged strain can be obtained by one particle embedded in the binder with the uniform binder's averaged strain. When the volume fraction of particles is fairly high or particles are clustered, even in the neighborhood of the particle other particles may exist, so the local field in the particle domain is highly distorted and the assumption of uniform strain field is not valid. Consequently, although MTM provides a better prediction than DM for most composites, for high volume fractions or a clustered microstructure, it produces a considerable disparity from the experimental results (Zheng and Du, 2001; Yin

et al., 2006). Moreover, the particle is still assumed to be spherical, so the effect of the particle shape is not considered.

Because the microstructure is statistically random, in the SCM, the averaged strain of the particle phase is represented by that at a randomly chosen infinitesimal material point as illustrated in Figure 1d. Because the point is so small, its effect on the effective material properties of the remaining material is negligible. Therefore, the particle's averaged strain can be obtained by a single infinitesimal particle embedded in the mastic itself under the uniform loading $\tilde{\sigma}^0$. Because the point can be chosen at any location in the particle phase, this model is applicable for general composites with irregular shapes and high volume fractions of particles.

It is noted that, in these three models, if the particle shape is ellipsoidal and the orientation is unified, using the solution for one ellipsoidal particle embedded in an infinite binder may provide a more accurate prediction (Zheng and Du, 2001). The connection between these models can be found in Yin and Sun (2005).

Because the neighboring material plays a more important role on the local strain field of a particle than the far field material does, GSCM uses the solution for a two layered particle embedded in the mastic itself to obtain the particle averaged strain. Compared to the self-consistent method, although the local interaction between the particle and the matrix is considered, the assumption of the spherical shape of the particle and the binder layer is imposed, which is not valid for asphalt mastics.

Overall, because filler particles are generally angular, flat, or sub-rounded, whereas DM, MTM, and GSCM are based on the assumption of spherical particles, the accuracy of these models is questionable. Although SCM does not consider the interaction between binders and particles, it offers some flexibility for the particle shape and volume fraction. Especially, when the volume fraction of particles is fairly high, the angular particles may contact with each other and form a skeleton. It is not feasible to see two layered particles in the mastics. SCM could be a good candidate model for such situation. Notice that all these models are based on the solution for one particle embedded in the infinite domain, so neither the effect of particle's shape and gradation nor the direct interaction between particles is considered (Yin *et al.*, 2006b; Buttlar *et al.*, 1999).

Because microstructures of asphalt mastics greatly change with material sources, gradation and volume fraction of filler particles, and material fabrication methods, the accuracy and applicability of each model needs to be validated by experiments.

5. Evaluation and comparison with experiments

To investigate the viscoelastic behavior of asphalt mastics at low temperatures, Di Benedetto *et al.* (2006) developed a uniaxial tension-compression test to measure both the complex Young's modulus (\tilde{E}) and the complex Poisson's ratio ($\tilde{\nu}$) of asphalt binders, mastics, and mixtures. Thus, the corresponding bulk modulus and

shear modulus can be calculated from isotropic material constant relations. In the test (Di Benedetto *et al.*, 2006), a 50/70 penetration grade asphalt binder and the corresponding mastic formulated with 32% well-graded limestone filler with a maximum particle size of 100 microns were tested. The frequencies of applied loading vary from 0.03 to 10 Hz (6 frequencies). The binder was tested at low temperatures, namely 0, -10, -15, -20, and -25°C. The tested complex Young's modulus and Poisson's ratio, seen in Appendix B, were found to be highly frequency and temperature dependent. Specifically, the absolute value of complex Poisson's ratio covers a broad range from 0.34 to 0.5. At high temperatures and low frequencies, it is reasonable to treat the binder as an incompressible material. However, at low temperatures and high frequencies, the compressibility of the binder was found to be non-negligible. In addition, the phase angles of the Poisson's ratio were found to be slightly negative in the range from 0 to -1.8°.

Once the binder's viscoelastic behavior is known, micromechanical models can be used to predict the effective viscoelastic properties of the corresponding asphalt mastics for different volume fractions. The tests of asphalt mastics were conducted at ENTP Laboratory (Di Benedetto *et al.*, 2006) at four temperatures such as 0, -10, -20, and -30 °C. First, we assume that the filler particles are rigid. Using the measured properties of the binder, the complex bulk modulus and shear modulus are estimated from four micromechanical models, namely, Equations [13], [18], [25] and [26], and [29] and [31], respectively. Thus, the complex Young's modulus and Poisson's ratio can be computed using

$$\langle \tilde{E} \rangle_D = \frac{9\langle \tilde{k} \rangle_D \langle \tilde{\mu} \rangle_D}{3\langle \tilde{k} \rangle_D + \langle \tilde{\mu} \rangle_D}, \quad \langle \tilde{\nu} \rangle_D = \frac{3\langle \tilde{k} \rangle_D - 2\langle \tilde{\mu} \rangle_D}{6\langle \tilde{k} \rangle_D + 2\langle \tilde{\mu} \rangle_D}. \quad [32]$$

The phase angle of these complex quantities can be obtained by their polar forms.

Assuming particles to be rigid, Figure 2 shows the predictions of the effective Young's moduli by four models compared with the experimental results at three temperatures. DM and SCM overestimates the experimental results; whereas GSCM and MTM underestimates the experimental results. Actually, Buttlar *et al.* (1999) and Shashidhar and Shenoy (2002) also observed that GSCM greatly underestimates the effective complex shear modulus in their experiments. Buttlar *et al.* (1999) introduced a rigid layer to interpret the physicochemical effect along the interface between particles and the binder. Shashidhar and Shenoy (2002) incorporated the concepts of percolation theory to modify GSCM and thus to fit the experiments. Although both papers finally produced good agreement with the experiments, they introduced some fitting parameters, which increased the complexity and uncertainty of the models. The validation of those parameters is still open. However, it is reiterated that the GSCM was developed for composites containing spherical particles (Christensen, 1990); whereas the filler particles of asphalt mastics typically have a very irregular shape.

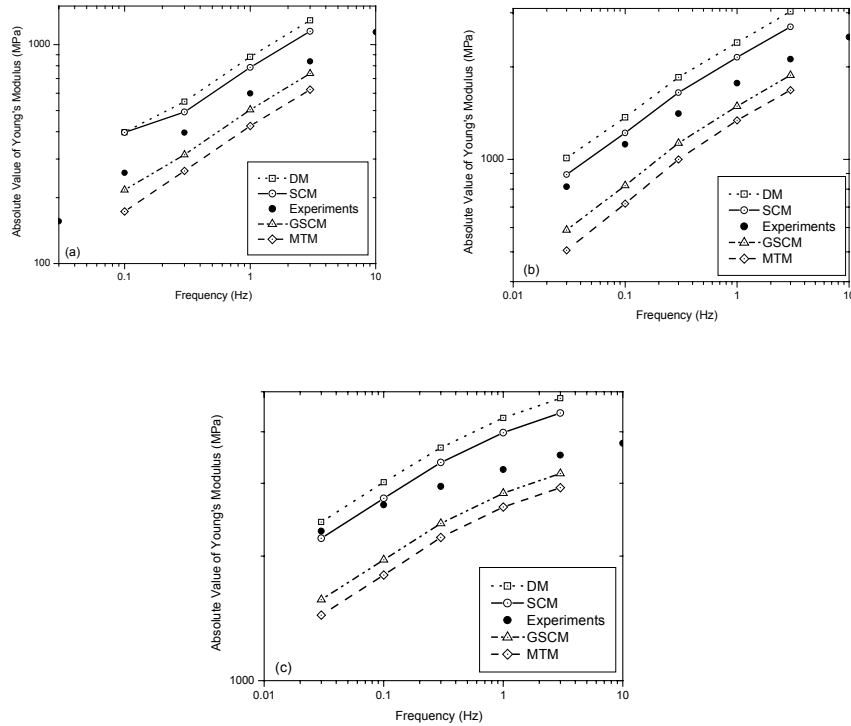


Figure 2. Comparison of the predictions of the effective Young's modulus with experimental results for the asphalt mastics measured at three temperatures: (a) 0 °C, (b) -10 °C, and (c) -20 °C. The filler particles are assumed to be rigid in the micromechanical models

Although the filler particles are typically much stiffer than the binder, at low temperatures, the stiffness of the binder is fairly high. The assumption of rigid particles may therefore not be suitable. Hence, the filler particles are herein treated as elastic materials. The Young's modulus of limestone was measured as 56.0GPa (Zhou *et al.*, 1995), and the Poisson's ratio is used as 0.3 (typically in the range of 0.2-0.3). Figure 3 illustrates the prediction of SCM compared with the measured values for the absolute values and phase angles of the complex Young's modulus of the asphalt mastics. Overall, the SCM is found to be in very good agreement with experimental results. Notice that no adjustable parameters are introduced. Here we do not illustrate the other three models because they provide much worse predictions, which can be projected from Figure 2. We can also see this fact in the comparison with another experiment.

Buttlar *et al.* (1999) tested the effective shear modulus of asphalt mastics containing different volume fractions of hydrated lime and baghouse filler particles, respectively. First, using the assumptions of the incompressible binder and the rigid filler particles, the effective shear modulus can be obtained from Equations [14], [19], [27], and [30] and [31] for the four models, respectively. It is noted that under the two assumptions, the phase angles of the shear modulus of asphalt binders are the same as those of the corresponding mastics. Figure 4a shows the shear modulus ratio of mastics to the binder for the tests. It can be found that GSCM and MTM considerably underestimate the experiments; whereas SCM and DM provide identical predictions, which lie between the experimental results for the two types of fillers. Due to the physicochemical effect between the hydrated lime filler and the binder, it has been suggested that there exists an adsorbed layer along the interface (Buttlar *et al.*, 1999; Little and Petersen, 2005), which is much stiffer than the pure binder. Thus, we can see that the tested shear moduli for the hydrated lime mastics are higher than the SCM predictions. Because particles are not really rigid, it is reasonable that the SCM overestimates the stiffness for the mastics with baghouse fillers.

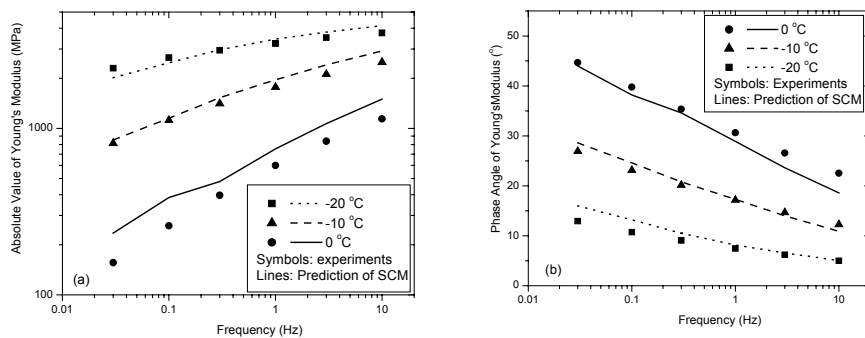


Figure 3. Comparison of the prediction of the Young's modulus by the self-consistent model with experimental results: (a) absolute value and (b) phase angle of the effective Young's modulus. The filler particles are considered as elastic materials

To produce a new prediction for the mastics with baghouse fillers using the present model, the following material properties were used: for the filler particles, $E^1 = 55.2\text{GPa}$ and $\nu^1 = 0.15$; and for the asphalt binder, $|\tilde{\mu}^0| = 177.6\text{MPa}$ and $\tilde{\nu}^0 = 0.4$. Because the asphalt binder is viscoelastic, the phase angle of the Poisson's ratio is chosen as zero, and that for the shear modulus is chosen as 0, 60, and 90° for the sake of parametric investigation. In Figure 4b, the SCM provides a fairly good prediction for the experimental results. Because the stiffness of the filler

is two orders of magnitude higher than that of the binder, the phase angle of the shear modulus of the binder does not produce a very large effect on the absolute value of the effective shear modulus of the mastics. However, it can still be observed that curve for the phase angle 90° is slightly higher than those with lower phase angles across most of the range of volume fractions.

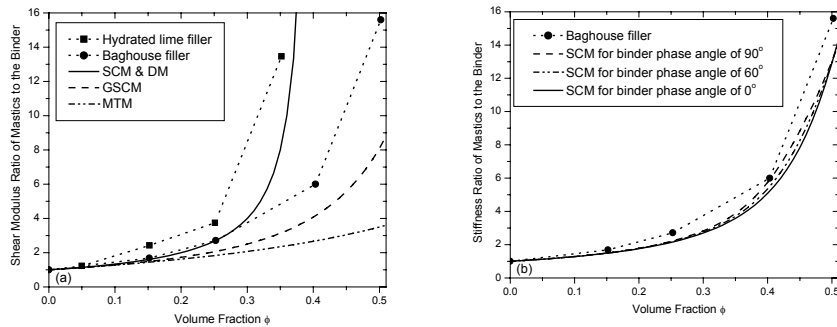


Figure 4. Prediction of effective Young's modulus and experimental results for asphalt mastic. (a) Rigid particles and incompressible binders used in the comparison of four models, and; (b) SCM predictions of baghouse filler mastic with parametric study of binder phase angles

To comprehensively study the effect of the phase angle of binder's stiffness on the effective stiffness of mastics, both the absolute value and the phase angle of effective Young's modulus of the mastics are illustrated in Figure 5, changing with the phase angle of Young's modulus of the binder. Herein, the following material properties were used: for the filler particles, $E^1 = 56$ GPa and $\nu^1 = 0.3$ (the same as those in Figure 3); and for the asphalt binder, $|\tilde{E}^0| = 1077$ MPa, and $|\tilde{\nu}^0| = 0.41$ and its phase angle $\theta^v = -1.3^\circ$ (selected from Appendix B). The phase angle of the Young's modulus for the binder θ^E is chosen as 0 , 30 , and 60° for the sake of parametric study. Figure 5 illustrates that although the absolute value of the Young's modulus of the binder keeps constant, the absolute value of the effective Young's modulus may change considerably with the phase angle of the Young's modulus of the binder. Moreover, because the filler particles are elastic, *i.e.* the phase angle of Young's modulus is equal to zero, the phase angle of the effective Young's modulus decreases along with the increase of the volume fraction of filler particles. Kim and Little (Kim *et al.*, 2004) also observed this phenomenon in their experiments with asphalt mastics containing limestone and hydrated lime fillers.

Figure 5 demonstrates that for two binders with the same absolute value of Young's modulus, if their phase angles are different, the effective viscoelastic behavior of the corresponding mastics will be different even using the same design. However, the previous models (for example, see Buttlar *et al.*, 1999; Shashidhar and

Shenoy, 2002; Kim and Little, 2004) take the absolute value of complex moduli as the corresponding elastic moduli, and use the formulation for an elastic model to predict the effective material properties. As a result, these models will always yield the same prediction as long as the absolute value of the binder's stiffness is the same, so they can neither capture the effect of the phase angle of the binder's stiffness, nor predict the phase angle of the effective stiffness, thereby limiting their accuracy.

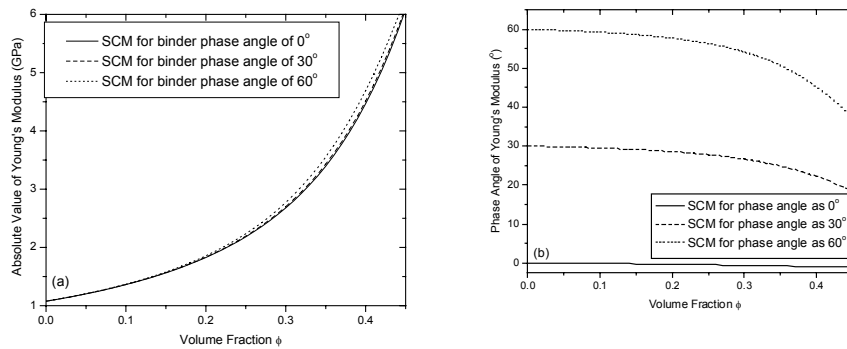


Figure 5. Effect of the phase angle of binder's Young's modulus on the effective Young's modulus of the mastics. (a) Absolute value and (b) phase angle of the effective complex Young's modulus

Certain asphalt binders, particularly neat binders, have been found to be thermorheologically simple (Anderson *et al.*, 1994), and thus the time-temperature superposition principle can be applied. Di Benedetto *et al.* (2004) used the classical WLF law (Ferry, 1980) to shift the data and found that the binder and mastic had very close shift factors for the complex Young's modulus and Poisson's ratio and the corresponding phase angles. For demonstrative purposes, the shift factor provided by Di Benedetto *et al.* (2004, 2006) is employed herein:

$$\log(a_T) = -\frac{24.5 \times T}{141.0 + T} \quad [33]$$

where T represents test temperature in °C. The reference temperature is then 0°C. It is noted that if individual shift factors are used for each case, more consistent master curves can be obtained, however; such analysis is beyond the current scope of this paper. Using the three dimensional expression of the 2S2P1D model proposed by Di Benedetto *et al.* (2006), the complex Young's modulus and the complex Poisson's ratio of the asphalt binder can be described as

$$\tilde{E}^0(\omega) = \frac{2.4}{1 + 2.3 \times (i0.003 \times 2\pi\omega)^{-0.21} + (i0.003 \times 2\pi\omega)^{-0.55} + (i0.003 \times 450 \times 2\pi\omega)^{-1}}$$

$$\tilde{\nu}^0(\omega) = 0.5 + (0.36 - 0.5) \frac{\tilde{E}^0(\omega)}{2.4}$$
[34]

which is shown in Figure 6 by the dotted line. Using the above equations and $E^1 = 56 \text{ GPa}$ and $\nu^1 = 0.3$ for the filler elastic properties, the effective Young's modulus of the asphalt mastics with 32% filler particles are calculated at different frequencies using Equations [24] and [32]. The absolute value and phase angles of the effective Young's modulus are illustrated in Figure 6, which agree with the experimental results quite well.

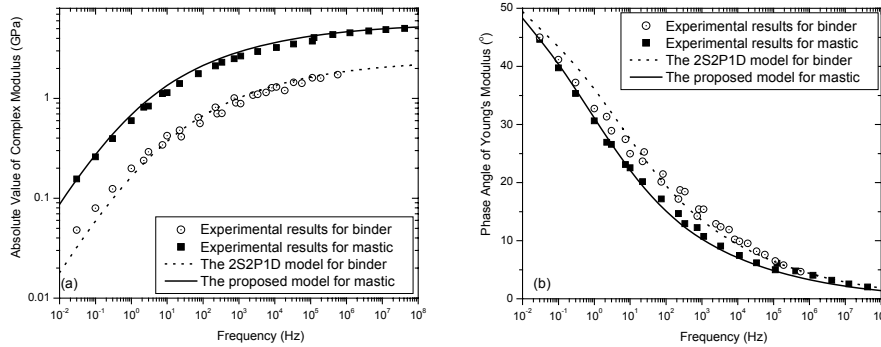


Figure 6. The master curves of the asphalt binder and mastic with experimental results. (a) absolute value of the Young's modulus, (b) phase angle of the Young's modulus. Reference temperature is 0°C

Given the viscoelastic behavior of binders and elastic properties of fillers, for the sake of material design, the SCM can be used to construct predicted master curves of effective complex modulus at any volume fraction, which can then be used to choose a favorable volume fraction. For instance, using the binder master curve model given by Equations [33] and [34], Figure 7 shows the predicted versus measured master curves for a range of asphalt mastics having volume fraction of filler particles of 0, 15%, 30%, 40%, and 45%. Because filler particles have much higher stiffness and much lower phase angle (namely, zero) compared to the binder, as the volume fraction of particles increases the absolute value of the effective complex Young's modulus increases, while the phase angle decreases. When the volume fraction is larger than 30%, the phase angle reduces very abruptly, which implies that the viscous effect is greatly reduced. In particular, the shape of the phase angle versus frequency relationship is significantly different at $\phi = 45\%$, as

the phase angle is predicted to increase with frequency, reaches a peak, and then decreases. This is logical, since at such a high volume fraction of mastic, for very low frequencies, the binder is extremely compliant and therefore the filler particles play a dominant role on the effective mechanical behavior. Thus, the effective phase angle is close to zero. At high frequencies, the stiffness of binder is high, and therefore the viscous effect of the binder becomes considerable, and the effective phase angle increases. When frequencies reach a certain point, the phase angle of the binder decreases, so that the effective phase angle decreases again.

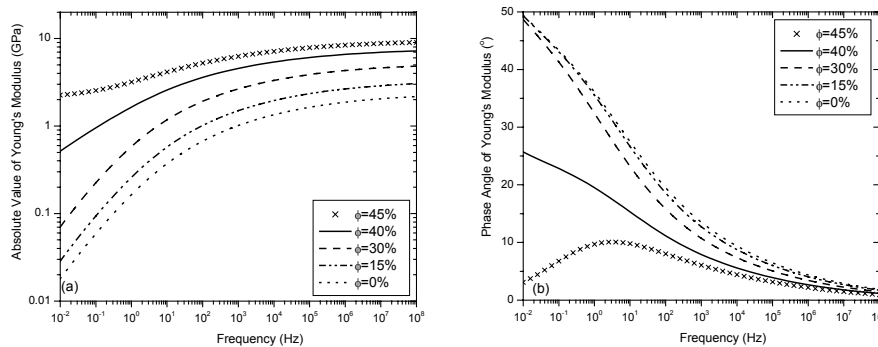


Figure 7. The master curves of asphalt mastics for different volume fractions. (a) absolute value of the complex Young's modulus, (b) phase angle

Because the SCM only depends on the volume fraction and material properties of individual constituents, but does not precisely consider the microstructure, for a specific sample of material, the effective viscoelastic properties may show some disparities from the prediction due to morphological, physicochemical, and gradation-related effects. Image processing techniques have provided a realistic approach to characterize actual microstructures (Masad *et al.*, 1999). By combining this information with numerical methods, the effective material behavior can be simulated (You, 2004; Abbas *et al.*, 2004). However, these approaches require rather laborious physical testing programs, and the simulation results depends on the size of samples, quality of meshing, discretization aspects, etc. Thus, the approach is generally very time-consuming and in the end, the results still contain uncertainties. The SCM represents a simple analytical method, which can quickly provide effective material properties, often with acceptable accuracy for the purposes of material design and/or analysis. It is hoped that the work can be extended to allow prediction of asphalt concrete mixture viscoelastic properties in the near future.

6. Conclusions

Four micromechanical models are formulated for the prediction of viscoelastic moduli of asphalt mastics. Given the viscoelastic properties of the binder and the elastic properties and volume fraction of the filler, the effective properties of the mastic are obtained. Through analyzing the simplifications and limitations of these models and comparing the predicted results with laboratory tests, the following conclusions are reached:

- The self-consistent model provides the best prediction for asphalt mastics, the Mori-Tanaka model and the generalized self-consistent model considerably underestimate the viscoelastic properties, while the dilute model greatly overestimates the experimental results.
- Conventional assumptions of incompressible binders and rigid fillers may not be valid for asphalt mastics at low temperatures. Using the actual material constants, the SCM approach produced an excellent prediction.
- The SCM approach shows that the phase angle for complex shear modulus of asphalt binders differ from that of the corresponding mastics. Thus, the previous employed elastic models, which neglect the effect of phase angle, is not able to fully capture the viscoelastic behavior of asphalt mastics.

Acknowledgements/Disclaimer

This work is sponsored by Federal Highway Administration National Pooled Fund Study 776, whose support is gratefully acknowledged. The results and opinions presented herein are those of the authors and do not necessarily reflect those of the sponsoring agency.

7. Bibliography

- Abbas A.R., Papagiannakis A.T. and Masad E.A., “Linear and nonlinear viscoelastic analysis of the microstructure of asphalt concretes”, *Journal of Materials in Civil Engineering*, Vol. 16, No. 2, 2004, p. 133-139.
- Anderson D.A., Christensen D.W., Bahia H.U., Dongre R., Sharma M.G., Antle C.E., and Button J., “Binder Characterization and Evaluation (SHRP A-369)”, Vol. 3 “Physical Characterization”, Strategic Highway Research Program, National Research Council, Washington DC, 1994.
- Airey G.D., Rahimzadeh B. and Collop A.C., “Linear rheological behavior of bituminous paving materials”, *Journal of Materials in Civil Engineering*, Vol. 16, No. 3, 2004, p. 212-220.
- Brinson L.C., Lin W.S., “Comparison of micromechanics methods for effective properties of multiphase viscoelastic composites”, *Composite Structures*, Vol. 41, No. 3-4, 1998, p. 353-367.

- Budiansky B., "On the elastic moduli of some heterogeneous materials", *Journal of the Mechanics and Physics of Solids*, 1965, 13, p. 223-227.
- Buttlar W.G., Bauer J.M., Sherman D.S., "Dynamic modulus of asphalt concrete with a hollow cylinder tensile tester", *Transportation Research Record* 1789, 2002, p. 183-190.
- Buttlar W.G., Bozkurt D., Al-Khateeb G.G. and Waldhoff A.S., "Understanding asphalt mastic behavior through micromechanics", *Transportation Research Record*, 1681, 1999, p. 157-166.
- Buttlar W.G. and Roque R., "Evaluation of Empirical and Theoretical Models to Determine Asphalt Mixture Stiffnesses at Low Temperatures", *Journal of Association of Asphalt Paving Technologists.*, 65, 1996, p. 99-130.
- Christensen D.W. and Anderson D.A., "Interpretation of Dynamic Mechanical Test Data for Paving Asphalt Cements", *Proceedings of the Association of Asphalt Paving Technologists*, 61, 1992, p. 67-116.
- Christensen R.M., "Viscoelastic properties of heterogeneous media", *Journal of the Mechanics and Physics of Solids*, 17, 1969, p. 23-41.
- Christensen R.M., *Theory of viscoelasticity: An introduction*, Academic Press, New York, 1982.
- Christensen R.M., "A critical evaluation for a class of micromechanics models", *Journal of Mechanics and Physics of Solids*, 38, 1990, p. 379-404.
- Christensen R.M. and Lo K.H., "Solutions for effective shear properties in three phase sphere and cylinder models", *Journal of the Mechanics and Physics of Solids*, 27, 1979, p. 315-330.
- Di Benedetto H., Olard F., Sauzéat C., and Delaporte B., "Linear viscoelastic behavior of bituminous materials: from binders to mixes", *EATA Nottingham, International Journal of Road Materials and Pavement Design*, Vol. 5, Special Issue, 2004, p. 163-202.
- Di Benedetto H., Delaporte B., and Sauzéat C., "Three-dimensional linear behavior of bituminous materials: experiments and modeling", *ASCE international Journal of Geomechanics*, Vol. 7, No. 2, p. 149-157, 2007
- Eshelby J.D., "The determination of the elastic field of an ellipsoidal inclusion, and related problems", *Proceedings of Royal Society A*, 241, 1957, p. 376-396.
- Eshelby J.D., "The elastic field outside an ellipsoidal inclusion", *Proceedings of Royal Society A*, 252, 1959, p. 561-569.
- Ferry J.D., *Viscoelastic properties of polymers*, 3rd Ed. Wiley, New York, 1980.
- Fung Y.C., *Foundations of solid mechanics*, Prentice-Hall, Englewood Cliffs, NJ, 1965.
- Gibiansky L.V., Milton G.W., "On the effective viscoelastic moduli of two-phase media. I. Rigorous bounds on the complex bulk modulus", *Proceedings of Royal Society London A*, 440, 1993, p. 163-188
- Gilormini P., Montheillet F., "Deformation of an inclusion in a viscous matrix and induced stress concentrations", *Journal of the Mechanics and Physics of Solids*, 34, 1986, p. 97-123.

- Haj-Ali R.M., Muliana A.H., "Micromechanical constitutive framework for the nonlinear viscoelastic behavior of pultruded composite materials", *International Journal of Solids and Structures*, 40, 2003, p. 1037-1057.
- Hashin, Z., "Viscoelastic behavior of heterogeneous media", *Journal of Applied Mechanics*, No. 32, 1965, p. 630-636.
- Hashin, Z., "Complex moduli of viscoelastic composites: I. General theory and application to particulate composites", *International Journal of Solids and Structures*, 6, 1970, p. 539-552.
- Hashin, Z. and Shtrikman S., "A variational approach to the theory of the elastic behavior of multiphase materials", *Journal of the Mechanics and Physics of Solids*, 11, 1963, p. 127-140.
- Herve E. and Zaoui A., "N-layered inclusion-based micromechanical modeling", *International Journal of Engineering Science*, 31, 1993, p. 1-10.
- Hill R., "A self-consistent mechanics of composite materials", *Journal of the Mechanics and Physics of Solids*, 13, 1965, p. 213-222.
- Kim Y.R., Lee Y.C., Lee H.J., "Correspondence principle for characterization of asphalt concrete", *Journal of Materials in Civil Engineering*, Vol. 7, No. 1, 1995, p. 59-68.
- Kim Y.R., Little D.N., "Linear viscoelastic analysis of asphalt mastics", *Journal of Materials in Civil Engineering*, 16, 2004, p. 122-132.
- Lackner R., Spiegl M., Blab R., Eberhardsteiner J., "Is low-temperature creep of asphalt mastic independent of filler shape and mineralogy? Arguments from multiscale analysis", *Journal of Materials in Civil Engineering*, Vol. 17, No. 5, 2005, p. 485-491.
- Laws N. and Mclaughlin R., "Self-consistent estimates for the viscoelastic creep compliances of composite materials", *Proceedings of Royal Society London A*, 359, 1978, p. 251-273
- Li J., Weng G.J., "A unified approach from elasticity to viscoelasticity to viscoplasticity of particle-reinforced solids", *International Journal of Plasticity*, 14, 1998, p. 193-208.
- Little D.N. and Petersen J.C., "Unique effects of hydrated lime filler on the performance-related properties of asphalt cements: physical and chemical interactions revisited", *Journal of Materials in Civil Engineering*, Vol. 17, No. 2, 2005, p. 207-218.
- Masad E., Muhunthan B., Shashidhar N., Harman T., "Internal Structure Characterization of Asphalt Concrete Using Image Analysis", *Journal of Computing in Civil Engineering*, Vol. 13, No. 2, 1999, p. 88-95.
- Milton G.W., Berryman J.G., "On the effective viscoelastic moduli of two-phase media. I. Rigorous bounds on the complex shear modulus in three dimensions", *Proceedings of Royal Society London A*, 453, 1997, p. 1849-1880.
- Mori T., Tanaka K., "Average stress in matrix and average elastic energy of materials with misfitting inclusions", *Acta Metallurgica*, 21, 1973, p. 571-574.
- Mukherjee S., Paulino G.H., "The elastic-viscoelastic correspondence principle for functionally graded materials, revisited", *Journal of Applied Mechanics*, 70, 2003, p. 359-363.

- Mura T., *Micromechanics of defects in solids*, 2nd Ed. Kluwer Academic Publishers, Dordrecht, 1987.
- Nemat-Nasser S., Hori M., *Micromechanics: Overall Properties of Heterogeneous Materials*, 2nd Edition, North-Holland. Amsterdam, 1999.
- Palade L.I., Attane P., Camaro S., “Linear viscoelastic behavior of asphalt and asphalt based mastic”, *Rheologica Acta*, 39, 2000, p. 180-190.
- Park S.W., Kim Y.R., “Interconversion between relaxation modulus and creep compliance for viscoelastic solids”, *Journal of Materials in Civil Engineering*, Vol. 11, No. 1, 1999, p. 76-82.
- Paulino G.H., Jin Z.H., “Correspondence principle in viscoelastic functionally graded materials”, *Journal of Applied Mechanics*, 68, 2001, p. 129-132.
- Ponte Castaneda P., Suquet P., “Nonlinear composites”, *Advances in Applied Mechanics*, 34, 1998, p. 171-302.
- Shashidhar N., Shenoy A., “On using micromechanical models to describe dynamic mechanical behavior of asphalt mastics”, *Mechanics of Materials*, 34, 2002p. 657-669.
- You Z., Buttlar W.G., “Discrete element modeling to predict the modulus of asphalt concrete mixtures”, *Journal of Materials in Civil Engineering*, Vol. 16, No. 2, 2004, p. 140-146.
- Yin H.M., Buttlar W.G., Paulino G.H., Di Benedetto H., “Micromechanics-Based Model for Asphalt Mastics Considering Viscoelastic Effects”, *10th International Conference on Asphalt Pavements*, 2006a.
- Yin H.M., Sun L.Z., “Magneto-elastic modeling of composites containing randomly dispersed ferromagnetic particles”, *Philosophical Magazine*, Vol. 86, No. 28, 2006b, p. 4367-4395.
- Yin H.M. and Sun L.Z., “Elastic modelling of periodic composites with particle interactions”, *Philosophical Magazine Letters*, 85, 2005, p. 163-173.
- Yin H.M., Sun L.Z., Paulino G.H., “Micromechanics-based elastic modeling for functionally graded materials with particle interactions”, *Acta Materialia*, 52, 2004, p. 3535-3543.
- Zheng Q.S., Du D.X., “An explicit and universally applicable estimate for the effective properties of multiphase composites which accounts for inclusion distribution”, *Journal of the Mechanics and Physics of Solids*, 49, 2001, p. 2765-2788.
- Zhou F.P., Lydon F.D., Barr B.I.G., “Effect of coarse aggregate on elastic modulus and compressive strength of high performance concrete”, *Cement and Concrete Research*, 25, 1995, p. 177-186.

Received: 3 January 2007

Accepted: 16 July 2007

8. Appendix

A. Correspondence principle and viscoelastic solution

Consider a single, spherical particle embedded in an infinite viscoelastic matrix with a uniform sinusoidal stress field as $\tilde{\boldsymbol{\sigma}}^0 e^{i2\pi\omega t}$. Without any loss of generality, we set the origin of coordinate at the center of the particle. For the given frequency ω , the constitutive relations for both the particle and the matrix in frequency domain can be written as

$$\tilde{\boldsymbol{\sigma}}(\mathbf{r}) = \begin{cases} \mathbf{C}^1 : \tilde{\boldsymbol{\varepsilon}}(\mathbf{r}) & \mathbf{r} \in \Omega \\ \tilde{\mathbf{C}}^0 : \tilde{\boldsymbol{\varepsilon}}(\mathbf{r}) & \mathbf{r} \in D - \Omega \end{cases} \quad [35]$$

Because the loading rate is relatively low, the loading is assumed to be quasi-static and thus dynamic force is not considered (Anderson *et al.*, 1994). The equilibrium equation is written as

$$\tilde{\sigma}_{ij,j}(\mathbf{r}) = 0. \quad [36]$$

The strain-displacement relation provides

$$\tilde{\varepsilon}_{ij}(\mathbf{r}) = \frac{1}{2} (\tilde{u}_{i,j} + \tilde{u}_{j,i}). \quad [37]$$

In the far field, the effect of the particle will be attenuated and the far field stress becomes

$$\tilde{\boldsymbol{\sigma}}(\mathbf{r}) = \tilde{\boldsymbol{\sigma}}^0, \quad \mathbf{r} \rightarrow \infty. \quad [38]$$

Along the interface of particle and matrix, the displacement and traction force should be continuous, so the continuity conditions give

$$\tilde{\mathbf{u}}^+ - \tilde{\mathbf{u}}^- = 0; \quad (\tilde{\boldsymbol{\sigma}}^+ - \tilde{\boldsymbol{\sigma}}^-) \cdot \mathbf{I} = 0; \quad \mathbf{r} \in \partial\Omega \quad [39]$$

where the superscripts + and – denote the inner and outer surface of the interface, respectively, and \mathbf{I} denotes the outward absolute value vector of the interface.

Equations [35]-[39] provide the governing equations and boundary conditions for the problem of one particle embedded in the infinite viscoelastic matrix. It is clear that they have the exact same form as the elastic problem except that these equations are in the complex domain whereas the elastic problem is in the real domain (Mura, 1987). Therefore, using the Green's function technique, this problem can be mathematically solved in the same fashion as the elastic problem. It is noted

that the correspondence principle is also valid for viscoelastic particle with replacing \mathbf{C}^1 in Equation [35] by $\tilde{\mathbf{C}}^1$.

Using the equivalent inclusion method, Eshelby (1957, 1959) has obtained the exact elastic solution for one ellipsoidal particle embedded in the infinite domain. Using his result, the viscoelastic solution for one spherical particle embedded in a viscoelastic binder can also be obtained. The local strain field in the matrix is written as

$$\tilde{\boldsymbol{\varepsilon}}(\mathbf{r}) = \tilde{\boldsymbol{\varepsilon}}^0 - \mathbf{P}(\mathbf{r}) \cdot (\mathbf{P}^0 - \Delta \tilde{\mathbf{C}}^{-1})^{-1} : \tilde{\boldsymbol{\varepsilon}}^0 \quad [40]$$

where

$$\tilde{\boldsymbol{\varepsilon}}^0 = (\tilde{\mathbf{C}}^0)^{-1} : \tilde{\boldsymbol{\sigma}}^0, \quad [41]$$

$$\Delta \tilde{\mathbf{C}} = \mathbf{C}^1 - \tilde{\mathbf{C}}^0, \quad [42]$$

$$P_{ijkl}^0 = \frac{1}{15\tilde{\mu}^0} \left[\frac{3\tilde{k}^0 + \tilde{\mu}^0}{3\tilde{k}^0 + 4\tilde{\mu}^0} \delta_{ij}\delta_{kl} - \frac{9}{2} \frac{\tilde{k}^0 + 2\tilde{\mu}^0}{3\tilde{k}^0 + 4\tilde{\mu}^0} (\delta_{ik}\delta_{jl} + \delta_{il}\delta_{jk}) \right], \quad [43]$$

and

$$P_{ijkl}(\mathbf{r}) = \frac{(3\tilde{k}^0 + \tilde{\mu}^0)\rho^3}{30\tilde{\mu}^0(3\tilde{k}^0 + 4\tilde{\mu}^0)} \left[\begin{array}{l} (5 - 3\rho^2)\delta_{ij}\delta_{kl} - \left(\frac{15\tilde{\mu}^0}{3\tilde{k}^0 + \tilde{\mu}^0} + 3\rho^2 \right) (\delta_{ik}\delta_{jl} + \delta_{il}\delta_{jk}) \\ -15(1 - \rho^2)(\delta_{ij}n_k n_l + \delta_{kl}n_i n_j) \\ -15 \left(\frac{3\tilde{k}^0 - 2\tilde{\mu}^0}{6\tilde{k}^0 + 2\tilde{\mu}^0} - \rho^2 \right) (\delta_{ik}n_j n_l + \delta_{il}n_j n_k + \delta_{jk}n_i n_l + \delta_{jl}n_i n_k) \\ +15(5 - 7\rho^2)n_i n_j n_k n_l \end{array} \right] \quad [44]$$

in which $\mathbf{n} = \mathbf{r}/|\mathbf{r}|$ and $\rho = a/|\mathbf{r}|$ (Yin *et al.*, 2004). The strain field in the particle is still uniform and written as Equation [5].

B. The complex young's modulus and Poisson's ratio of the asphalt BINDER

Temperature	Frequency	$ \tilde{E}^0 $	θ^E	$ \tilde{\nu}^0 $	θ^{ν}
(°C)	(Hz)	(MPa)	(°)		(°)
0°C	0.03				
	0.1	79.57	41.17	0.50	-0.18
	0.3	124.21	37.21	0.48	-0.49
	1	199.14	32.74	0.48	-0.79
	3	292.26	28.92	0.48	-1.29
	10	422.73	24.97		
-10°C	0.03	239.17	31.35	0.47	-0.59
	0.1	341.81	27.45	0.46	-0.82
	0.3	479.69	23.66	0.45	-0.97
	1	645.67	20.14	0.44	-1.20
	3	813.69	17.17	0.44	-1.55
	10	1008.16	14.24		
-15°C	0.03	412.89	25.27	0.44	-1.09
	0.1	561.99	21.47	0.43	-0.99
	0.3	704.38	18.72	0.42	-0.95
	1	904.76	15.42	0.41	-1.05
	3	1077.23	12.90	0.41	-1.30
	10	1282.55	10.22		
-20°C	0.03	710.42	18.43	0.41	-1.68
	0.1	886.09	15.41	0.41	-1.30
	0.3	1099.03	12.37	0.40	-1.25
	1	1299.82	9.89	0.40	-1.24
	3	1452.50	8.18	0.40	-1.30
	10	1606.39	6.51		
-25°C	0.03	1149.95	11.92	0.38	-1.78
	0.1	1199.09	9.54	0.34	-0.93
	0.3	1420.39	7.61	0.35	-1.05
	1	1597.19	5.80	0.36	-0.94
	3	1734.93	4.67	0.36	-1.12
	10				